SPE Paper Number 97731

Stabilization of Gas Distribution Instability in Single Point Dual Gas-Lift Wells

Gisle Otto Eikrem, SPE, Ole Morten Aamo, and Bjarne A. Foss, Norwegian University of Science and Technology

Abstract

While casing-heading instability in single gas-lift wells has attracted a lot of attention, gas distribution instability in *dual* gas-lift wells has not. In this paper, we present a simple nonlinear dynamic model which is shown to capture the essential dynamics of the gas distribution instability despite the complex nature of two-phase flow. Using the model, stability maps are generated showing regions of stable and unstable settings for the production valves governing the produced flows from the two tubings. Optimal steady state production is shown to lie well within the unstable region, corresponding to a gas distribution between the production tubings that cannot be sustained without automatic control. A simple control structure is suggested that successfully stabilizes the gas distribution instability in simulations, and more importantly in laboratory experiments.

1 Introduction

Artificial lift is a common technique to increase tail-end production from mature fields, and injection of gas (gas-lift) rates among the most widely used such methods. Gas-lift can induce severe production flow oscillations because of casing-heading instability, a phenomenon which originates from dynamic interaction between injection gas in the casing and the multiphase fluid in the tubing. The fluctuating flow typically has an oscillation period of a few hours and is distinctly different from short-term oscillations caused by hydrodynamic slugging. The casing-heading instability introduces two production-related challenges. Average production is decreased as compared to a stable flow regime, and the highly oscillatory flow puts strain on downstream equipment.

Reports from industry as well as academia suggest that automatic control (feedback control) is a powerful tool to eliminate casing-heading instability

and increase production from gas-lift wells[1-7]. Automatic control may or may not require downhole measurements. If downhole information is needed by the controller, the use of soft sensing techniques may alleviate the need for downhole measurements. In Aamo et al.[7], downhole pressure is estimated online using a simple dynamic model and measurements at the well head, only. The estimated pressure is in turn used in a controller for stabilizing the casing-heading instability.

Understanding and predicting under which conditions a gas-lift well will exhibit flow instability is important in every production planning situation. This problem has been addressed by several authors by constructing stability maps, i.e. a 2D diagram which shows the regions of stable and unstable production of a well[8,9]. The axes define the operating conditions in terms of the gas-injection rate and for instance the production choke opening or wellhead pressure.

A dual gas-lift well is a well with two independent tubings producing from two different hydrocarbon bearing layers, and sharing a common lift-gas supply. The injection gas is supplied through a common casing and injected into the tubings through two individual gas lift valves. A sketch of a typical system is shown in **Fig. 1**. The dual gas-lift well introduces a new instability phenomenon, the gas distribution instability. This relates to the fact that under certain operating conditions, it is impossible to sustain the feed of injected gas into both tubings. Instead, all the injected gas will eventually be routed through one of the gas-lift valves. As a consequence, the second tubing produces poorly, or not at all, decreasing the total production substantially. There are few reports, if any, on automatic control of dual gas-lift wells, although Boisard et al.[4] briefly mentions an application.

In this paper, we present a simple nonlinear dynamic model that captures the essential dynamics of the gas distribution instability. It is an extension of the model for a single gas lift-well presented in Eikrem et al.[6] and Aamo et al.[7] Using the model, we generate a stability map for a single point dual gas-lift well, and present a control structure for stabilizing the system at open-loop unstable setpoints. The performance of the controller is demonstrated in simulations using the model, but

more importantly, stabilization is also achieved in laboratory experiments.

The paper is organized as follows: In Section 2 a nonlinear dynamic model applicable to dual gas-lift wells is presented followed by a discussion on instability mechanisms and generation of stability maps in Section 3. The stability analysis is based on computing eigenvalues for the linearized model, accompanied by simulations using the nonlinear model. The proposed control structure is presented in Section 3.3, and experimental results using a gas-lift laboratory located at TU Delft are shown in Section 4. The paper ends with a discussion and some conclusions in Section 5.

2 Mathematical Model

The process described in the introduction, and sketched in Fig. 1, is modelled mathematically by five states: x_1 is the mass of gas in the annulus; x_2 is the mass of gas in tubing 1; x_3 is the mass of oil above the gas injection point in tubing 1; x_4 is the mass of gas in tubing 2, and; x_5 is the mass of oil above the gas injection point in tubing 2. Looking at Fig. 1, we have

$$\dot{x}_1 = w_{gc} - w_{iv,1} - w_{iv,2}, \quad \text{.....(1)}$$

$$\dot{x}_2 = w_{iv,1} + w_{rg,1} - w_{pg,1}, \quad \text{.....(2)}$$

$$\dot{x}_3 = w_{ro,1} - w_{po,1}, \quad \text{.....(3)}$$

$$\dot{x}_4 = w_{iv,2} + w_{rg,2} - w_{pg,2}, \quad \text{.....(4)}$$

$$\dot{x}_5 = w_{ro,2} - w_{po,2}. \quad \text{.....(5)}$$

where $\dot{}$ denotes differentiation with respect to time, and w_{gc} is a constant mass flow rate of lift gas into the annulus, $w_{iv,k}$ is the mass flow rate of lift gas from the annulus into tubing k, $w_{rg,k}$ is the gas mass flow rate from the reservoir into tubing k, $w_{pg,k}$ is the mass flow rate of gas through production choke k, $w_{ro,k}$ is the oil mass flow rate from the reservoir into tubing k, and $w_{po,k}$ is the mass flow rate of produced oil through production choke k ($k \in \{1,2\}$). The flows are modelled by

$$w_{gc} = \text{ constant flow rate of lift gas,} \quad \text{.....(6)}$$

$$w_{iv,1} = C_{iv,1}\sqrt{\rho_{a,i}\max\{0, p_{a,i} - p_{wi,1}\}}, \quad \text{.....(7)}$$

$$w_{iv,2} = C_{iv,2}\sqrt{\rho_{a,i}\max\{0, p_{a,i} - p_{wi,2}\}}, \quad \text{.....(8)}$$

$$w_{pc,1} = C_{pc,1}\sqrt{\rho_{m,1}\max\{0, p_{wh,1} - p_s\}}\, f_{pc,1}(u_1), \quad \text{.....(9)}$$

$$w_{pc,2} = C_{pc,2}\sqrt{\rho_{m,2}\max\{0, p_{t,2} - p_s\}}\, f_{pc,2}(u_2), \quad \text{...(10)}$$

$$w_{pg,1} = \frac{x_2}{x_2 + x_3} w_{pc,1}, \quad \text{.....(11)}$$

$$w_{po,1} = \frac{x_3}{x_2 + x_3} w_{pc,1}, \quad (12)$$

$$w_{pg,2} = \frac{x_4}{x_4 + x_5} w_{pc,2}, \quad (13)$$

$$w_{po,2} = \frac{x_5}{x_4 + x_5} w_{pc,2}, \quad (14)$$

$$w_{ro,1} = f_{r,1}(p_{r,1} - p_{wb,1}), \quad (15)$$

$$w_{ro,2} = f_{r,2}(p_{r,2} - p_{wb,2}), \quad (16)$$

$$w_{rg,1} = r_{go,1} w_{ro,1}, \quad (17)$$

$$w_{rg,2} = r_{go,2} w_{ro,2}. \quad (18)$$

$C_{iv,k}$ and $C_{pc,k}$ are constants, u_k is the production choke setting ($u_k(t) \in [0,1]$), $\rho_{a,i}$ is the density of gas in the annulus at the injection point, $p_{a,i}$ is the pressure in the annulus at the injection point, $\rho_{m,k}$ is the density of the oil/gas mixture at the well head, $p_{wh,k}$ is the pressure at the well head, $p_{wi,k}$ is the pressure in the tubing at the gas injection point, $p_{wb,k}$ is the pressure at the well bore, p_s is the pressure in the manifold, $p_{r,k}$ is the reservoir pressure far from the well, and $r_{go,k}$ is the gas-to-oil-ratio (based on mass flows) of the flow from the reservoir. The function $f_{pc,k}$ is valve specific and represents a possibly nonlinear scaling of the flow as a function of the choke setting u_k. $f_{r,k}$ is a case specific, possibly nonlinear, mapping from the pressure difference between the reservoir and the well bore to the fluid flow from the reservoir. The manifold pressure, p_s, is assumed to be held constant by a control system, and the reservoir pressure, $p_{r,k}$, and gas-to-oil-ratio, $r_{go,k}$, are assumed to be slowly varying and therefore treated as constant. Note that flow rates through the valves are restricted to be positive. The densities are modelled as follows

$$\rho_{a,i} = \frac{M}{RT_a} p_{a,i}, \quad (19)$$

$$\rho_{m,k} = \frac{x_{1+k} + x_{2+k}}{L_{w,k} A_{w,k}}, \quad (20)$$

and the pressures as follows

$$p_{a,i} = \left(\frac{RT_a}{V_a M} + \frac{gL_a}{V_a} \right) x_1, \quad (21)$$

$$p_{wh,k} = \frac{RT_{w,k}}{M} \frac{x_{1+k}}{L_{w,k} A_{w,k} - \nu_o x_{2+k}}, \quad (22)$$

$$p_{wi,k} = p_{wh,k} + \frac{g}{A_{w,k}} (x_{1+k} + x_{2+k}), \quad (23)$$

$$p_{wb,k} = p_{wi,k} + \rho_o g L_{r,k}. \quad (24)$$

M is the molar weight of the gas, R is the gas constant, T_a is the temperature in the annulus, $T_{w,k}$ is the temperature in the tubing, V_a is the volume of the annulus, L_a is the length of the annulus, $L_{w,k}$ is the length of the tubing, $A_{w,k}$ is the cross sectional area of the tubing above the injection point, $L_{r,k}$ is

the length from the reservoir to the gas injection point, $A_{r,k}$ is the cross sectional area of the tubing below the injection point, g is the gravity constant, ρ_o is the density of the oil, and v_o is the specific volume of the oil. The oil is considered incompressible, so $\rho_o=1/v_o$ is constant. The temperatures, T_a and $T_{w,k}$ are slowly varying and therefore treated as constant. This model is an extension to dual-well from the single-well model presented in Eikrem et al.[6] and Aamo et al.[7]

3 Instability Mechanisms and Control

3.1 Casing Heading Instability. The dynamics of highly oscillatory flow in single point injection gas-lift wells can be described as follows:

1. Gas from the annulus starts to flow into the tubing. As gas enters the tubing the pressure in the tubing falls, accelerating the inflow of lift-gas.
2. If there is uncontrolled gas passage between the annulus and tubing, the gas pushes the major part of the liquid out of the tubing, while the pressure in the annulus falls dramatically.
3. The annulus is practically empty, leading to a negative pressure difference over the injection orifice blocking the gas flow into the tubing. Due to the blockage, the tubing becomes filled with liquid and the annulus with gas.
4. Eventually, the pressure in the annulus becomes high enough for gas to penetrate into the tubing, and a new cycle begins.

For more information on this type of instability, often termed severe slugging, the reader is referred to Xu and Golan[10]. The oscillating production associated with severe slugging causes problems for downstream processing equipment, and is unacceptable in operations. The traditional remedy is to choke back to obtain a non-oscillating flow. As mentioned in the Introduction, automatic control is a powerful approach to eliminate oscillations. Moreover, reports also show that this technology increases production[1-7]. Another approach is to fit a gas-lift valve which secures critical flow. This decouples the dynamics of the casing and tubing volumes and thereby eliminates casing-heading instabilities. Since the topic of this paper is a different kind of instability present in dual gas-lift wells, we refer the reader to [1-7,10] for more details concerning stabilization of casing-heading instabilities.

3.2 Gas Distribution Instability. In single point dual gas-lift oil wells another instability mechanism related to the distribution of lift gas between the two tubings occurs. The following statements assume sub-critical flow between the annulus and the two tubings. Suppose each tubing is steadily drawing 50% of the lift gas. If one tubing momentarily draws more, the hydrostatic pressure drop in the tubing decreases, resulting in a larger pressure drop across the gas injection orifice. This in turns accelerates the flow of gas, and the tubing draws even more lift gas. On the other hand, since the gas flow into the second tubing decreases, the hydrostatic pressure drop in the second tubing increases. Thus, the pressure drop across the gas injection orifice decreases, and as a consequence, less gas is routed through the second tubing. Eventually, all lift gas will be routed through one tubing and this could impact total oil production.

We will now analyze gas distribution instability using the relatively simple model (1)-(5), applied to the gas-lift laboratory used in the experiments of Section 4. For the laboratory, we have

$$f_{pc,k}(u_k) = 50^{u_k - 1}, \quad \text{.....(25)}$$

$$f_{r,k}(p_{r,k} - p_{wb,k}) = C_{r,k}\sqrt{\rho_o \max\{0, p_{r,k} - p_{wb,k}\}}, \quad (26)$$

$k \in \{1,2\}$, where $C_{r,1}$ and $C_{r,2}$ are constants. Table 1 summarizes the numerical coefficients used for this case. Given a pair of production valve openings, u_1 and u_2 for the long and short tubing, respectively, we look for steady state solutions by setting the time derivatives in (1)-(5) to zero. Not all choices of u_1 and u_2 are feasible with respect to obtaining production from both tubings. The yellow *and* black dots in **Fig. 2** represent the pairs u_1 and u_2 whose steady state solution corresponds to production from both tubings. Other choices will give production from one tubing, only, and are not of interest to us. For the pairs of interest, we linearize system (1)-(5) around the steady state solution in order to study linear stability. The black dots in Fig. 2 represent (linearly) unstable settings. Roughly speaking, there is a region $(u_1, u_2) \in (0,0.50) \times (0,0.38)$ of linearly stable settings, while the rest are unstable settings. **Fig. 3** shows the steady state total production as a function of (u_1, u_2). Clearly, production is higher for large values of u_1 and u_2. In fact, the optimum is located approximately at (1.00,0.83), which corresponds to an unstable setting and a steady state production substantially larger than what can be achieved in the linearly stable region. The gas

distribution at steady state as a function of (u_1, u_2) is shown in **Fig. 4**.

For u_1 = 0.90 and u_2 = 0.83, the steady state solution is unstable, with the largest real part of the eigenvalues of the linearized system being strictly positive ($\max_j\{\mathrm{Re}(\lambda_j)\} = 0.03$). Selecting the initial condition equal to the steady state solution, only slightly perturbed, and simulating system (1)-(5), we obtain the result shown in **Figs. 5 and 6**. Fig. 5 shows the gas distribution between the two tubings as functions of time. At approximately steady state, 5/6 of the gas flows through the long tubing, while 1/6 of the gas flows through the short tubing. After about two minutes, the instability becomes visible in this graph, and the gas starts to redistribute. After about 13 minutes, all the gas is routed through the short tubing. Fig. 6 shows the corresponding fluid production curves. The long tubing has a substantial drop in production as a result of losing its lift gas, while the short tubing produces a little more. The total production drops about 20 %.

3.3 Automatic Control. To optimize production the instability needs to be dealt with. Motivated by the success of the controller used to stabilize the casing-heading instability, the control structure in **Fig. 7** is proposed. It consists of two independent feedback loops regulating the pressure at the injection points of each tubing. More precisely, two PI controllers (proportional gain plus integral action) are employed, producing the incremental control signals

$$\Delta u_k(j) = K_{c,k}\left(e_k(j) - e_k(j-1) + \frac{\Delta t}{\tau_{I,k}} e_k(j)\right), \quad \text{....(27)}$$

$k \in \{1,2\}$, where

$$e_k(j) = p_{wi,k}(j) - p^*_{wi,k} \quad \text{.....(28)}$$

$K_{c,k}$ and $\tau_{I,k}$ are the proportional gains and integral times, respectively, Δt is the sampling time, and j denotes the time index. $p^*_{wi,k}$, $k \in \{1,2\}$, are appropriate setpoints for the pressure. Repeating the simulation from Figs. 5 and 6, and closing the control loops at t = 10 minutes, we obtain the result in **Figs. 8 and 9.** Fig. 8 shows the gas distribution between the two tubings. At the time of initiation of control (t = 10), the gas has been considerably redistributed, but the control effectively drives the system back to the steady state solution. Fig. 9 shows the corresponding fluid production. The

control inputs that achieve this result are shown in **Fig. 10**.

4 Laboratory Experiments

Realistic tests of control structures for gas-lift wells are performed using the gas-lift well laboratory setup at TU Delft[♣]. Prior laboratory experiments have verified that the PI controller (27)-(28) successfully stabilizes the casing-heading instability in single gas-lift wells[6]. Motivated by that result, the same control structure is tested experimentally for stabilization of the gas distribution instability in dual gas-lift wells.

4.1 Experimental Setup. The laboratory installation represents a dual gas-lift well, using compressed air as lift-gas and water as produced fluid. It is sketched in Fig. 7. The two production tubes are transparent, facilitating visual inspection of the flow phenomena occurring as control is applied. The long tubing measures 18 m in height and has an inner diameter of 20 mm, while the short tubing measures 14 m in height and has an inner diameter of 32 mm, see **Fig. 11a**. Each tubing has its own fluid reservoir represented by a tube of the same height, but with the substantially larger inner diameters of 80 mm and 101 mm, respectively. The reservoir pressures are given by the static height of the fluid in the reservoir tubes. The top of the tubings are aligned, which implies that the long tubing stretches 4 meters deeper than the short one. A gas bottle represents the annulus, see Fig. 11b, with the gas injection points located at the same level in both tubings and aligned with the bottom of the short production tube, see Fig. 7. In the experiments run in this study, gas is fed into the annulus at a constant rate of 0.6×10^{-3} kg/s. Input and output signals to and from the installation are handled by a microcomputer system, see Fig. 11c, to which a laptop computer is interfaced for running the control algorithm and presenting output.

4.2 Experimental Results. For the prescribed rate of lift-gas, the two PI control loops sketched in Fig. 7 are incapable of stabilizing the gas distribution instability from an arbitrary initial condition, and in particular initial conditions for

[♣] The experimental setup is designed and implemented by Shell International Exploration and Production B.V., Rijswijk, and is now located in the Kramers Laboratorium voor Fysische Technologie, Faculty of Applied Sciences, Delft University of Technology.

which only one tubing is producing are not feasible ones. Therefore, a simple startup procedure, consisting of the following steps, was used in order to bring the system into a state from which the controller is able to stabilize:

1. Set u_1 and u_2 close to the expected steady state values. This does not have to be very accurate.
2. Momentarily increase the rate of lift-gas beyond the nominal rate (w_{gc}) such that both tubings draw gas and produce in open-loop.
3. While both tubings draw lift gas, close the control loops.
4. Gradually decrease the rate of lift-gas to its nominal value.

In the experiments, the coefficients for the controllers were set to $K_{c,1}$ = -1.2, $K_{c,2}$ = -1.5, and $\tau_{I,1} = \tau_{I,2}$ = 50 s, while the sampling time was Δt = 1.5 s. The setpoints for $p_{wi,1}$ and $p_{wi,2}$ were set equal to $p^*_{wi,1} = p^*_{wi,2} = 1$ barg (2 bar, 2×10^5 Pa), and the pressure deviations (28) were computed in barg (as opposed to Pa). **Figs. 12 and 13** show the controlled downhole pressures $p_{wi,1}$ and $p_{wi,2}$ as functions of time, along with the setpoints $p^*_{wi,1}$ and $p^*_{wi,2}$. The two PI control loops gradually drive $p_{wi,1}$ and $p_{wi,2}$ towards their respective setpoints, reaching them in about 8 minutes. The commanded production valve openings achieving this result are shown in **Figs. 14 and 15**. The valve openings are approximately 75% and 82% when regulation to setpoint is achieved. At t = 10 minutes, the control is turned off in order to demonstrate that the setpoints are indeed open-loop unstable. Figs. 12 and 13 show that the pressures diverge rapidly from their setpoints after t = 10 minutes, confirming open-loop instability. **Fig. 16** shows the gas distribution between the two tubings. During regulation, in the period between t = 8 and t = 10 minutes, about one third of the gas is routed through the short tubing while two thirds are routed through the long tubing. The uneven gas distribution for this case of identical setpoints ($p^*_{wi,1} = p^*_{wi,2}$) is due to the difference in valve characteristics between the two gas injection valves (see $C_{iv,1}$ and $C_{iv,2}$ in Table 1). Total production during regulation is about 10 kg/min, as shown in **Fig. 17**. The effect of the gas distribution instability is evident as control is turned off in the interval t = 10 to t = 15 minutes in Figs. 16 and 17. The gas quickly redistributes with 100% being routed through the short tubing and nothing through the long tubing. As a consequence, the long tubing

stops producing, while the short tubing produces a little more. The total production drops by about 28%, making a strong case for applying automatic control. Comparing the interval $t \in [10,15]$ in Figs. 16 and 17 to Figs. 5 and 6, the qualitative resemblance is striking when considering the highly complex nature of two-phase flow and the simplicity of the model of Section 2. While part of the difference between simulations and experiments is due to modelling error, the fact that simulations and experiments are performed at different setpoints is also a source of difference in this comparison. Although the model was set up for the laboratory case in this paper, it can easily be modified for real cases by changing parameters and reservoir flow relationships. In particular, $f_{r,1}(\cdot)$, $f_{r,2}(\cdot)$, $r_{go,1}$, and $r_{go,2}$ must be modified to model flows from a real reservoir. Typically, reservoir oil flow is modelled proportional (productivity index) to the pressure difference $p_{r,k}$ - $p_{wb,k}$, while the gas-to-oil ratio is usually treated as constant.

Additional experiments were run to determine whether just one of the control loops is sufficient for stabilization of the gas distribution instability. The experiments were unsuccessful, from which we conclude that both control loops are required. It is a drawback that the controllers rely on downhole measurements, since such measurements may not be available or unreliable. The use of soft sensing techniques may alleviate the need for downhole measurements, as demonstrated in Aamo et al.[7] In that reference, the downhole pressure was estimated online from measurements at the well head, only, and employed for stabilization of the casing-heading instability.

5 Conclusions

In this paper, we have presented a simple scheme for stabilization of the gas distribution instability in dual gas-lift oil wells with a common lift-gas supply. A simple nonlinear dynamic model, consisting of only five states, was shown to successfully capture the essential dynamics of the gas distribution instability despite the complex nature of two-phase flow. Using the model, stability maps were generated showing regions of linearly stable and unstable settings for the production valves governing the produced flows from the two tubings. Accompanying plots of total production indicated that optimal steady state production lies at

large valve openings, and well within the unstable region. A simple control structure was suggested that successfully stabilizes the gas distribution instability in simulations, and more importantly in laboratory experiments. For the settings used in the laboratory, total production dropped 28 % when automatic control was switched off! Comparing simulation results with experiments, the predictive capability of the model is evident.

The results of this paper show that the problem of gas distribution instability in dual gas-lift oil wells may be analyzed and counteracted by simple methods, and that there is a potential for significantly increasing production by installing a simple, inexpensive, control system.

Acknowledgements

We gratefully acknowledge the support from Shell International Exploration and Production B.V., and Kramers Laboratorium voor Fysische Technologie, Faculty of Applied Sciences, Delft University of Technology. In particular, we would like to thank Dr. Richard Fernandes (Shell) and Prof. Dr. R.V.A. Oliemans (TU Delft).

Nomenclature

$A_{r,1}$	Cross sectional area of tubing 1 below the gas injection point, [L^2], m^2
$A_{r,2}$	Cross sectional area of tubing 2 below the gas injection point, [L^2], m^2
$A_{w,1}$	Cross sectional area of tubing 1 above the gas injection point, [L^2], m^2
$A_{w,2}$	Cross sectional area of tubing 2 above the gas injection point, [L^2], m^2
$C_{iv,1}$	Valve constant for gas injection valve 1, [L^2], m^2
$C_{iv,2}$	Valve constant for gas injection valve 2, [L^2], m^2
$C_{pc,1}$	Valve constant for production valve 1, [L^2], m^2
$C_{pc,2}$	Valve constant for production valve 2, [L^2], m^2
$C_{r,1}$	Valve constant for reservoir valve 1, [L^2], m^2
$C_{r,2}$	Valve constant for reservoir valve 2, [L^2], m^2
Δt	Time step, [t], s
e_k	Regulation error, [m/Lt^2], Pa
g	Acceleration of gravity, [L/t^2], m/s^2
L_a	Length of annulus, [L], m

$L_{r,1}$ Length of tubing 1 below gas injection point, [L], m

$L_{r,2}$ Length of tubing 2 below gas injection point, [L], m

$L_{w,1}$ Length of tubing 1 above gas injection point, [L], m

$L_{w,2}$ Length of tubing 2 above gas injection point, [L], m

M Molar weight of gas, [m/n], kg/mol

ν_o Specific volume of oil, [L^3/m], m^3/kg

p_a Pressure at the gas injection point in the annulus, [m/Lt^2], Pa

$p_{r,1}$ Pressure in reservoir 1, [m/Lt^2], Pa

$p_{r,2}$ Pressure in reservoir 2, [m/Lt^2], Pa

p_s Pressure in the manifold, [m/Lt^2], Pa

$p_{wh,1}$ Pressure at well head 1, [m/Lt^2], Pa

$p_{wh,2}$ Pressure at well head 2, [m/Lt^2], Pa

$p_{wb,1}$ Pressure at well bore 1, [m/Lt^2], Pa

$p_{wb,2}$ Pressure at well bore 2, [m/Lt^2], Pa

$p_{wi,1}$ Pressure at gas injection point in tubing 1, [m/Lt^2], Pa

$p_{wi,2}$ Pressure at gas injection point in tubing 2, [m/Lt^2], Pa

R Universal gas constant, [mL^2/nTt^2], J/Kmol

$r_{go,1}$ Gas-to-oil ratio in flow from reservoir 1

$r_{go,2}$ Gas-to-oil ratio in flow from reservoir 2

$\rho_{a,i}$ Density of gas at injection point in annulus, [m/L^3], kg/m^3

$\rho_{m,1}$ Density of mixture at well head 1, [m/L^3], kg/m^3

$\rho_{m,2}$ Density of mixture at well head 2, [m/L^3], kg/m^3

ρ_o Density of oil, [m/L^3], kg/m^3

t Time, [t], s

T_a Temperature in annulus, [T], K

$T_{w,1}$ Temperature in tubing 1, [T], K

$T_{w,2}$ Temperature in tubing 2, [T], K

u_1 Setting of production valve 1

u_2 Setting of production valve 2

V_a Volume of annulus, [L^3], m^3

w_{gc} Flow of gas into annulus, [m/t], kg/s

$w_{iv,1}$ Flow of gas from annulus into tubing 1, [m/t], kg/s

$w_{iv,2}$ Flow of gas from annulus into tubing 2, [m/t], kg/s

$w_{pc,1}$ Flow of mixture from tubing 1, [m/t], kg/s

$w_{pc,2}$ Flow of mixture from tubing 2, [m/t], kg/s

$w_{po,1}$ Flow of oil from tubing 1, [m/t], kg/s

$w_{po,2}$ Flow of oil from tubing 2, [m/t], kg/s

$w_{pg,1}$ Flow of gas from tubing 1, [m/t], kg/s

$w_{pg,2}$ Flow of gas from tubing 2, [m/t], kg/s

$w_{ro,1}$ Flow of oil from reservoir into tubing 1, [m/t], kg/s

$w_{ro,2}$ Flow of oil from reservoir into tubing 2, [m/t], kg/s

$w_{rg,1}$ Flow of gas from reservoir into tubing 1, [m/t], kg/s

$w_{rg,2}$ Flow of gas from reservoir into tubing 2, [m/t], kg/s

x_1 Mass of gas in annulus, [m], kg

x_2 Mass of gas in tubing 1, [m], kg

x_3 Mass of oil in tubing 1, [m], kg

x_4 Mass of gas in tubing 2, [m], kg

x_5 Mass of oil in tubing 2, [m], kg

References

1. Kinderen, W.J.G.J., and Dunham, C.L.: "Real-time artificial lift optimization," paper SPE 49463 presented at the Abu Dhabi International Petroleum Exhibition and Conference, Abu Dhabi, United Arab Emirates, November 11-14, 1998.
2. Jansen, B., Dalsmo, M., Nøkleberg, L., Havre, K., Kristiansen, V., and Lemetayer, P.: "Automatic control of unstable gas lifted wells," paper SPE 56832 presented at the 1999 SPE Annual Technical Conference and Exhibition, Houston, Texas, USA, October 3-6.
3. Dalsmo, M., Halvorsen, E., and Slupphaug, O.: "Active feedback control of unstable wells at the Brage field," paper SPE 77650 presented at the 2002 SPE Annual Technical Conference and Exhibition, San Antonio, Texas, USA, September 29 – October 2.
4. Boisard, O., Makaya, B., Nzossi, A., Hamon, J.C., and Lemetayer, P.: "Automated well control increases performance of mature gas-lifted fields, Sendji case," paper SPE 78590 presented at the Abu Dhabi International Petroleum Exhibition and Conference, Abu Dhabi, United Arab Emirates, October 13-16, 2002.
5. Hu, B., and Golan, M.: "Gas-lift instability resulted production loss and its remedy by feedback control: dynamical simulation results," paper SPE 84917 presented at the SPE International Improved Oil Recovery Conference in Asia Pacific, Kuala Lumpur, Malaysia, October 20-21, 2003.

6. Eikrem, G.O., Imsland, L., and Foss, B.: "Stabilization of gas lifted wells based on state estimation," Proceedings of the International Symposium on Advanced Control of Chemical Processes, Hong Kong, China, 2004.
7. Aamo, O.M., Eikrem, G.O., Siahaan, H., and Foss, B.A.: "Observer design for multiphase flow in vertical pipes with gas-lift -- theory and experiments," *Journal of Process Control*, **15**, No. 1, pp. 247-257, 2005.
8. Poblano, E., Camacho, R., and Fairuzov, Y.V.: "Stability analysis of continuous-flow gas-lift wells," paper SPE 77732 presented at the 2002 SPE Annual Technical Conference and Exhibition, San Antonio, Texas, USA, September 29 – October 2.
9. Fairuzov, Y.V., Guerrero-Sarabia, I., Calva-Morales, C., Carmona-Diaz, R., Cervantes-Baza, T., Miguel-Hernandez, N., and Rojas-Figueroa, A.: "Stability maps for continuous gas-lift wells: a new approach to solving an old problem," paper SPE 90644 presented at the 2004 SPE Annual Technical Conference and Exhibition, Houston, Texas, USA, September 26-29.
10. Xu, Z.G., and Golan, M.: "Criteria for operation stability of gas-lift wells," paper SPE 19362 available from SPE, Richardson, Texas (1989).

SI Metric Conversion Factors

bar	×	1.0*	E+05	=	Pa
bbl	×	1.589 873	E-01	=	m^3
Btu	×	1.055 056	E+00	=	kJ
ft	×	3.048*	E-01	=	m
ft^2	×	9.290 304*	E-02	=	m^2
ft^3	×	2.831 685	E-02	=	m^3
°F		(°F+459.67)/1.8		=	K
lbm	×	4.535 924	E-01	=	kg

*Conversion factor is exact.

Table 1: Numerical coefficients.

Parameter	Value	Unit
M	0.028	kg/mol
R	8.31	J/Kmol
g	9.81	m/s^2
T_a	293	K
L_a	0.907	m
V_a	22.3×10^{-3}	m^3
ρ_o	1000	kg/m^3
p_s	1×10^{5}	Pa
w_{gc}	0.6×10^{-3}	kg/s
$p_{r,1}$	2.9×10^{5}	Pa
$T_{w,1}$	293	K
$L_{w,1}$	14	m
$L_{r,1}$	4	m
$A_{w,1}$	0.314×10^{-3}	m^2
$A_{r,1}$	0.314×10^{-3}	m^2
$C_{iv,1}$	1.60×10^{-6}	m^2
$C_{pc,1}$	0.156×10^{-3}	m^2
$C_{r,1}$	12×10^{-6}	m^2
$r_{go,1}$	0	-
$p_{r,2}$	2.5×10^{5}	Pa
$T_{w,2}$	293	K
$L_{w,2}$	14	m
$L_{r,2}$	0	m
$A_{w,2}$	0.804×10^{-3}	m^2
$A_{r,2}$	0.804×10^{-3}	m^2
$C_{iv,2}$	2.80×10^{-6}	m^2
$C_{pc,2}$	0.156×10^{-3}	m^2
$C_{r,2}$	0.15×10^{-3}	m^2
$r_{go,2}$	0	-

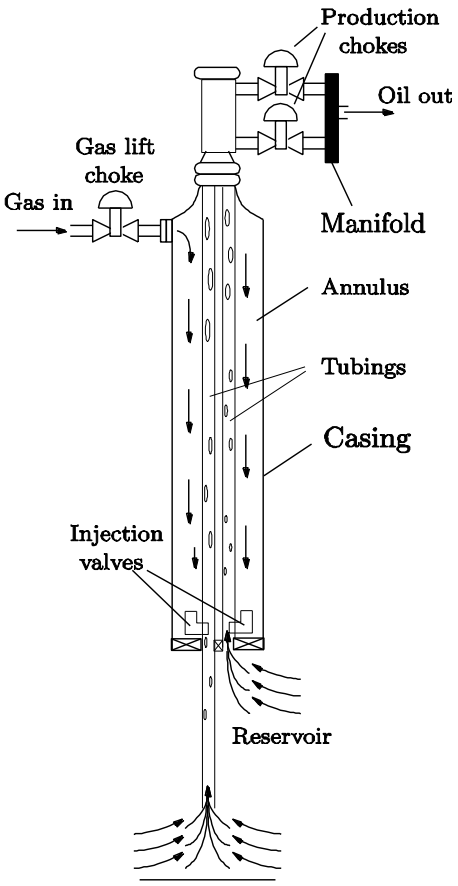

Fig. 1: A single point dual gas-lift oil well.

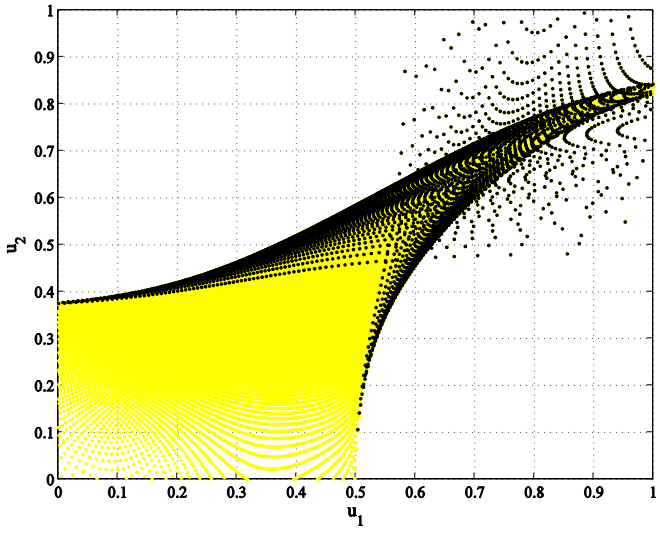

Fig. 2: Feasible choke settings for production from both tubings (yellow *and* black area), and choke settings for which open-loop production is unstable (black area).

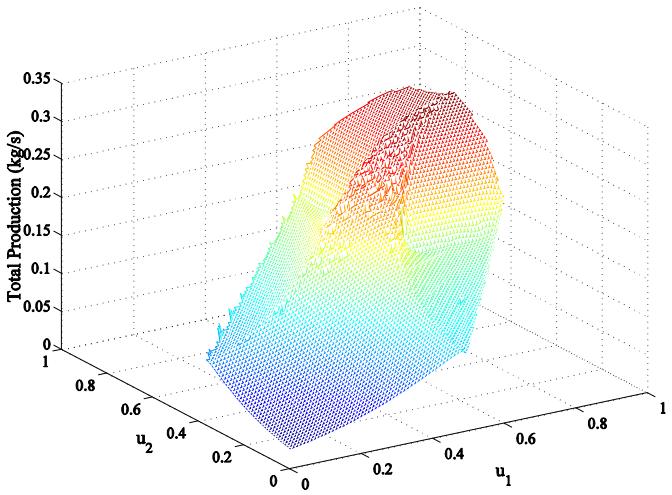

Fig. 3: Total fluid production as a function of u_1 and u_2.

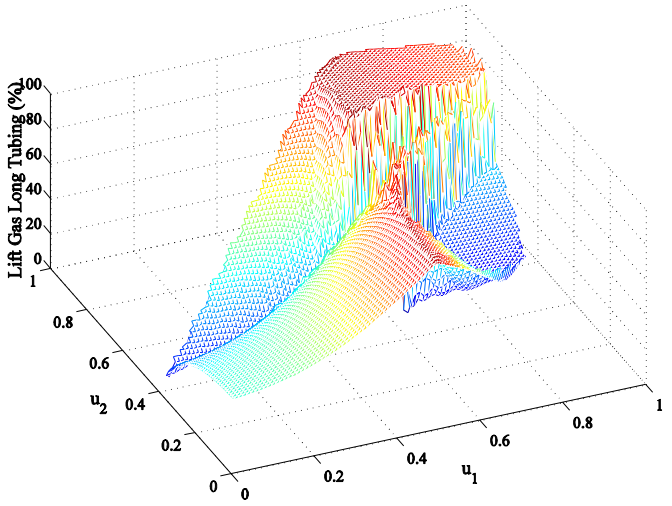

Fig. 4: Gas distribution as a function of u_1 and u_2.

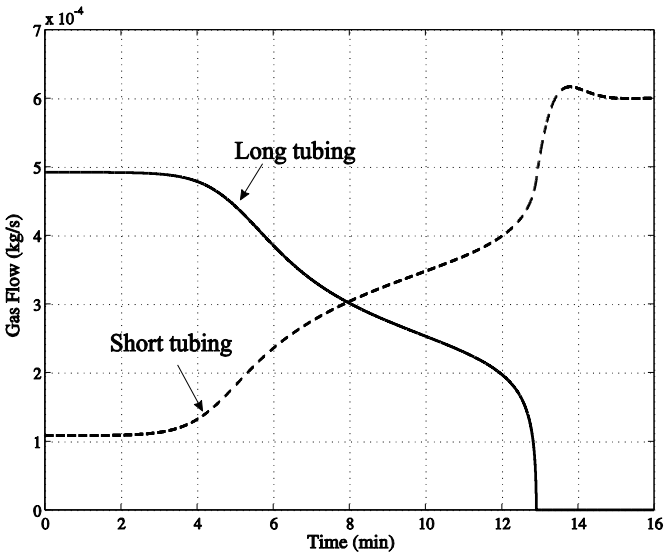

Fig. 5: Gas distribution as a function of time in the uncontrolled case.

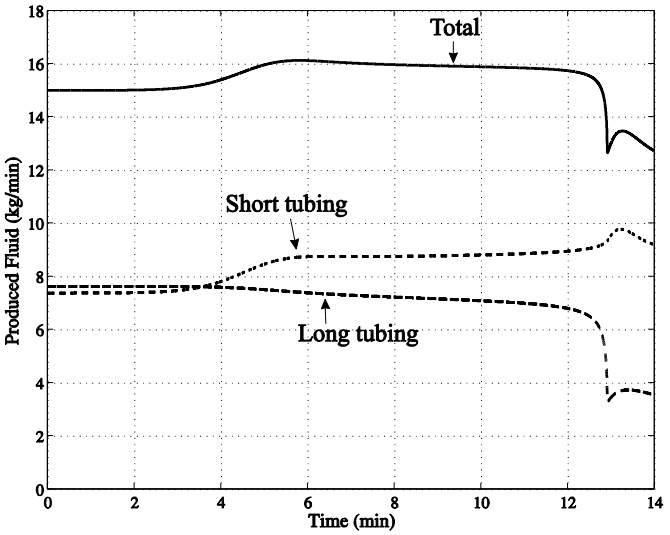

Fig. 6: Fluid production as a function of time in the uncontrolled case.

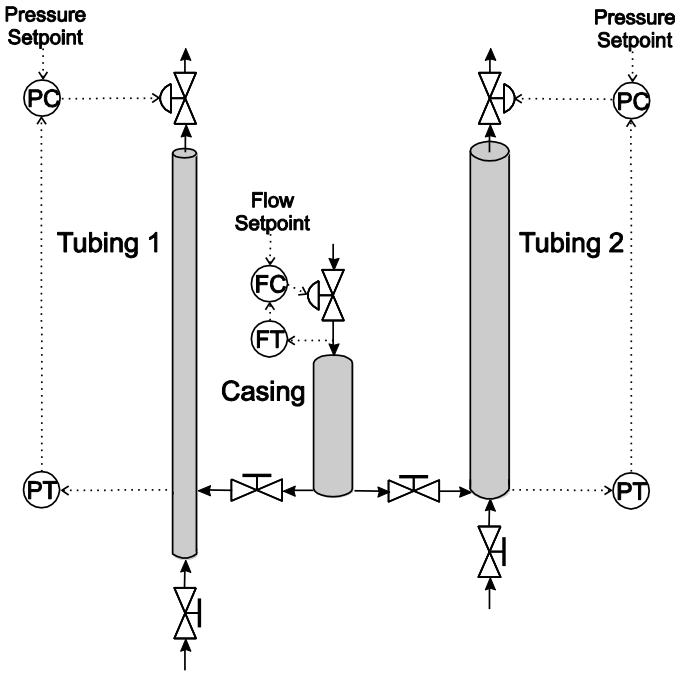

Fig. 7: Controller structure for stabilization of the gas distribution instability.

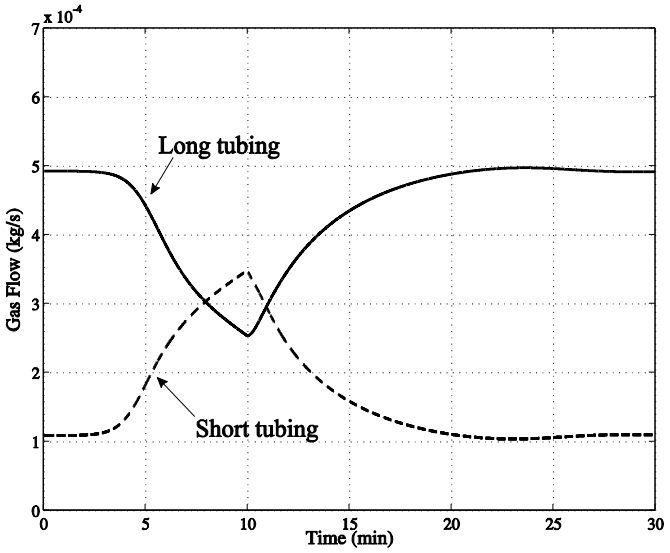

Fig. 8: Gas distribution as a function of time in the controlled case. Control is turned on at t = 10 minutes.

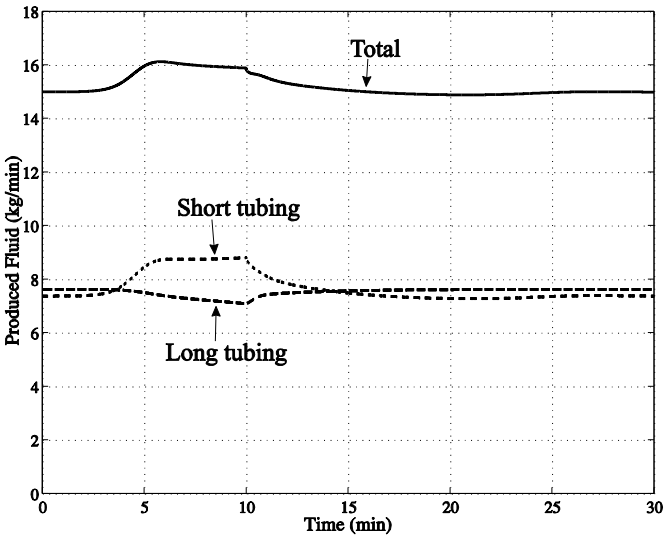

Fig. 9: Fluid production as a function of time in the controlled case. Control is turned on at t = 10 minutes.

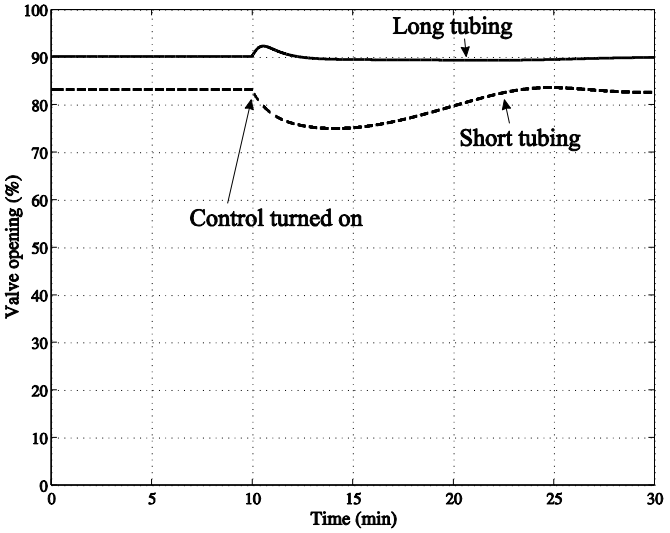

Fig. 10: Production valve openings as functions of time. Control is turned on at t = 10 minutes.

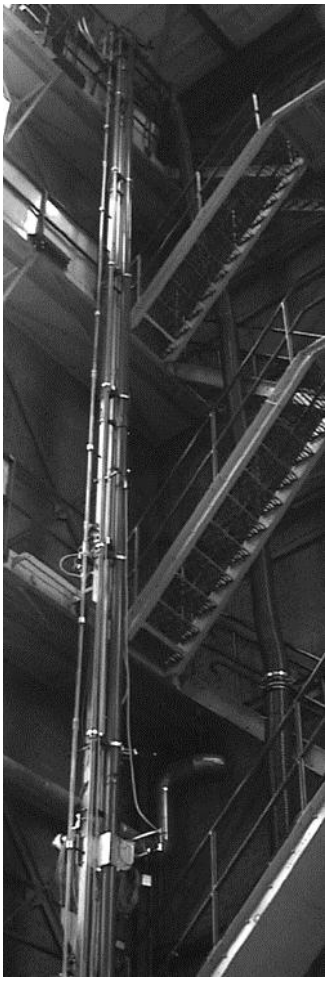

a) The production tubes.

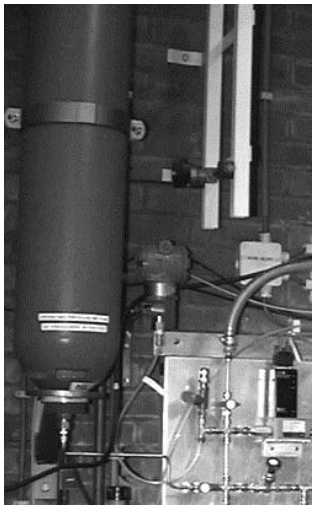

b) The annulus volume.

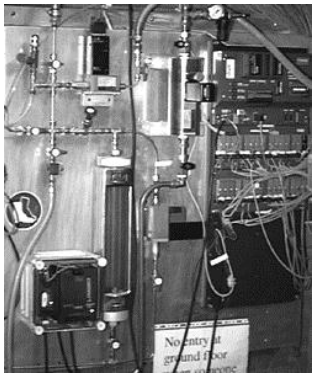

c) The microcomputer.

Fig. 11: The gas-lift laboratory.

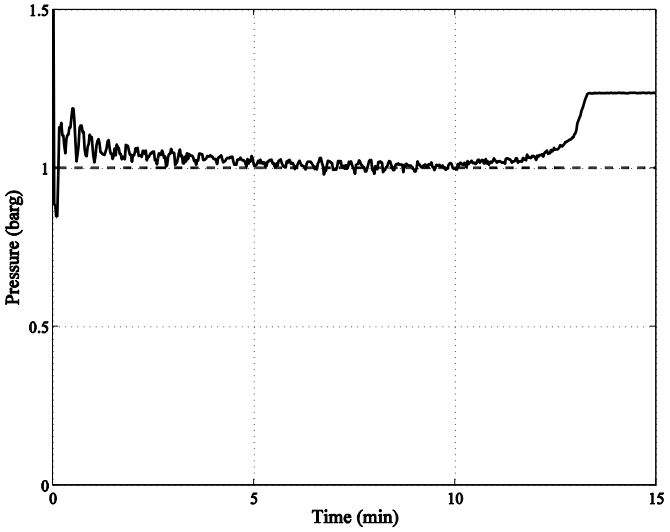

Fig. 12: Pressure at the location of gas injection in the long tubing. Control is turned off at t = 10 minutes. The dashed line specifies the setpoint $p^*_{wi,1}$.

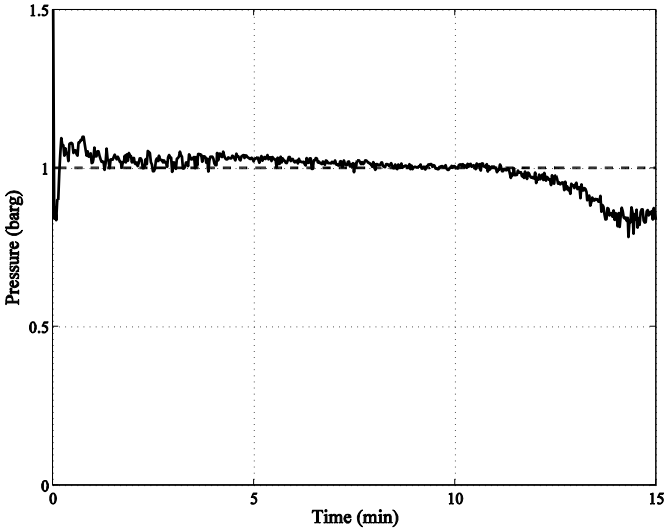

Fig. 13: Pressure at the location of gas injection in the short tubing. Control is turned off at t = 10 minutes. The dashed line specifies the setpoint $p^*_{wi,2}$.

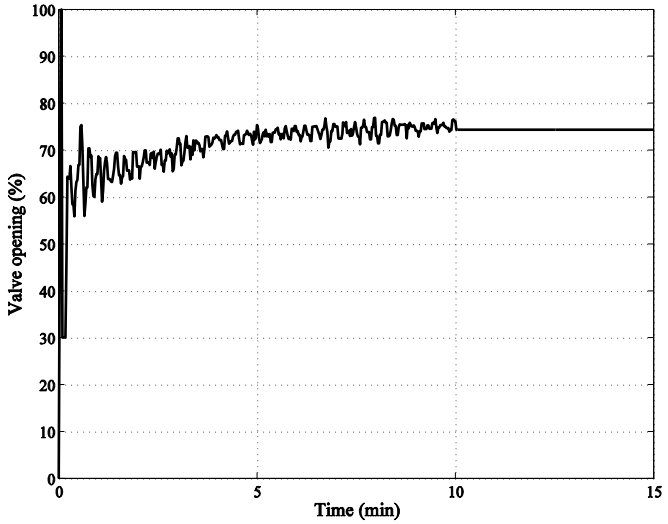

Fig. 14: Production valve opening for the long tubing. Control is turned off at t = 10 minutes, keeping the valve opening at the last controlled value.

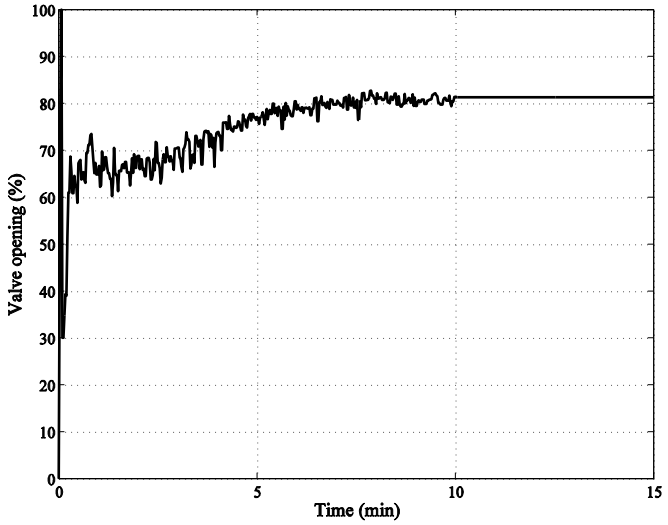

Fig. 15: Production valve opening for the short tubing. Control is turned off at t = 10 minutes, keeping the valve opening at the last controlled value.

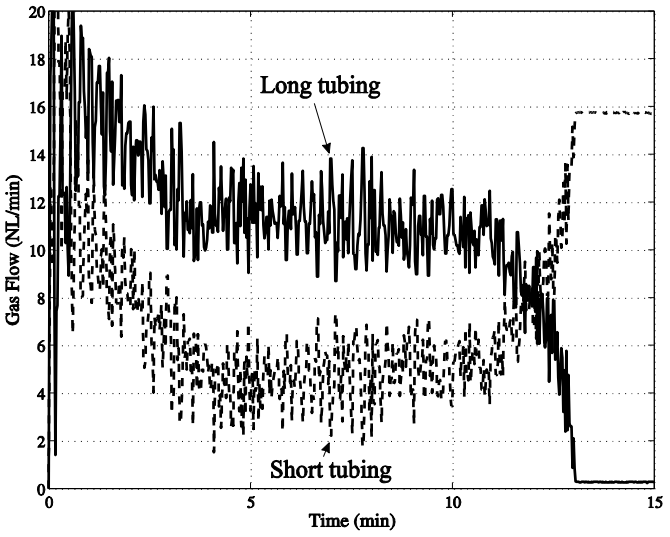

Fig. 16: Gas distribution as a function of time. Control is turned off at t = 10 minutes.

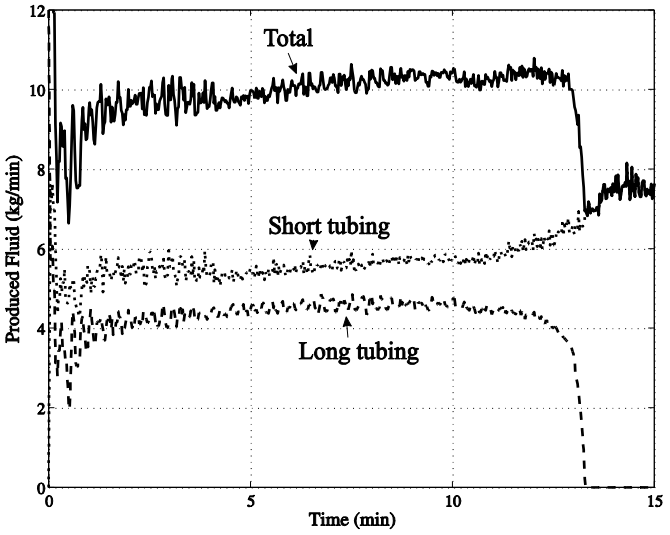

Fig. 17: Fluid production as a function of time. Control is turned off at t = 10 minutes.